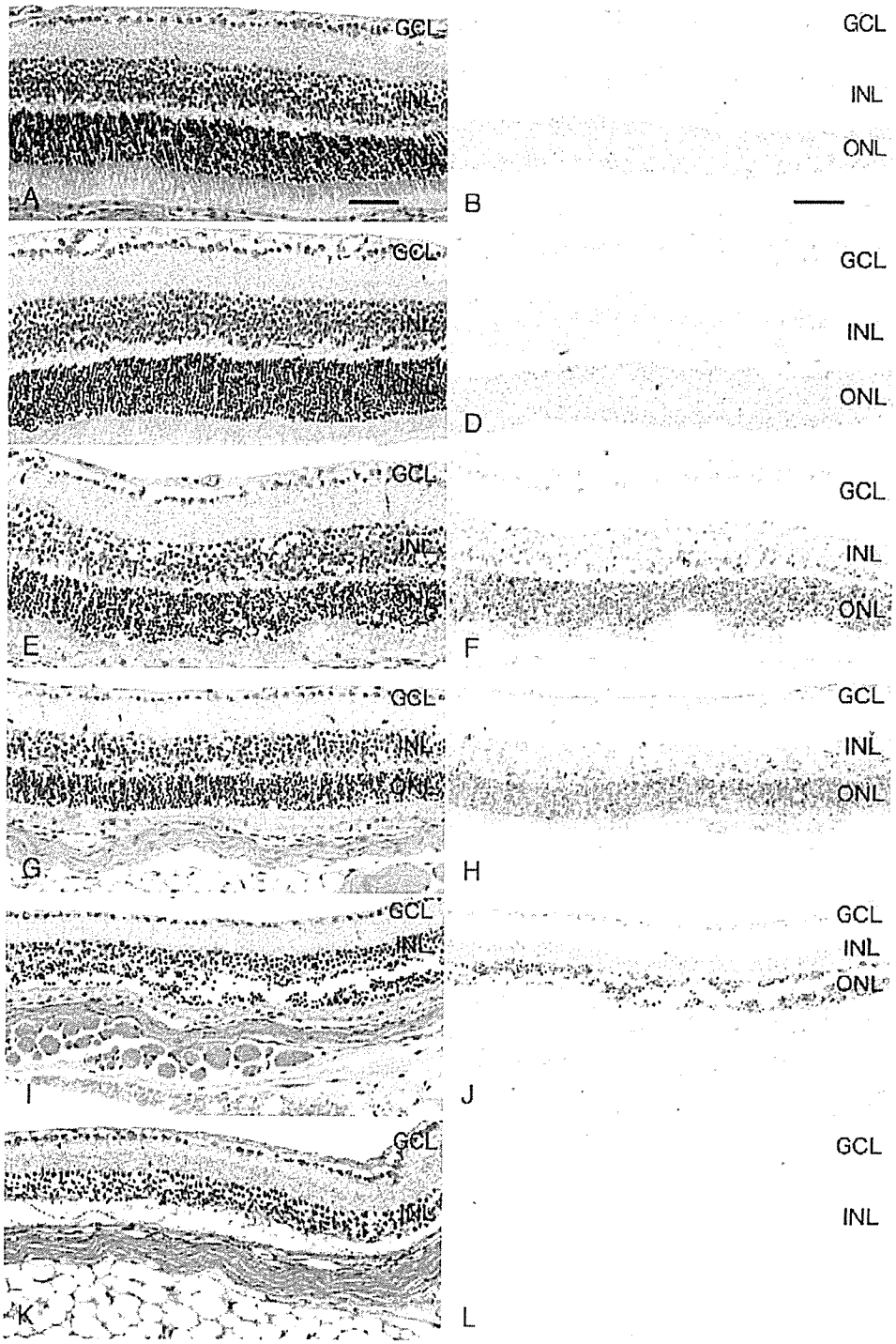

Fig. 2 – Time course analysis for mouse retina detected by hematoxylin and eosin staining (A, C, E, G, I, K) and TUNEL staining (B, D, F, H, J, L) at 12 (A, B), 24 (C, D), 48 (E, F) and 96 h (G, H) and 1 (I, J) and 2 weeks (K, L) after intravitreal cobalt chloride injection at the dose of 12 nmol. There is no morphological damage 12 and 24 h after intravitreal injection (A, C). No TUNEL-positive apoptotic cells are seen at 12 h (B), however, a few TUNEL-positive cells are seen at 24 h (D). TUNEL-positive cells peaked at 48 h after injection (F). Only small numbers of nuclei in ONL are seen at 1 week after the injection (I, J), and the ONL disappeared at 2 weeks (K, L). GCL, ganglion cell layer; INL, inner nuclear layer; ONL, outer nuclear layer. Scale bar in panels A and B, 50 μm.

outer nuclear layer (ONL) in retina, 1; atrophy of ONL, 2; disappearance of ONL, 3; and damage of total retinal layers, 4. Most severe lesion was evaluated and scored in each retina. The mean score of each group of cobalt-chloride-treated retina was defined as retinal damage index (RDI). Furthermore, photoreceptor damage rate (PDR) was defined as the ratio of

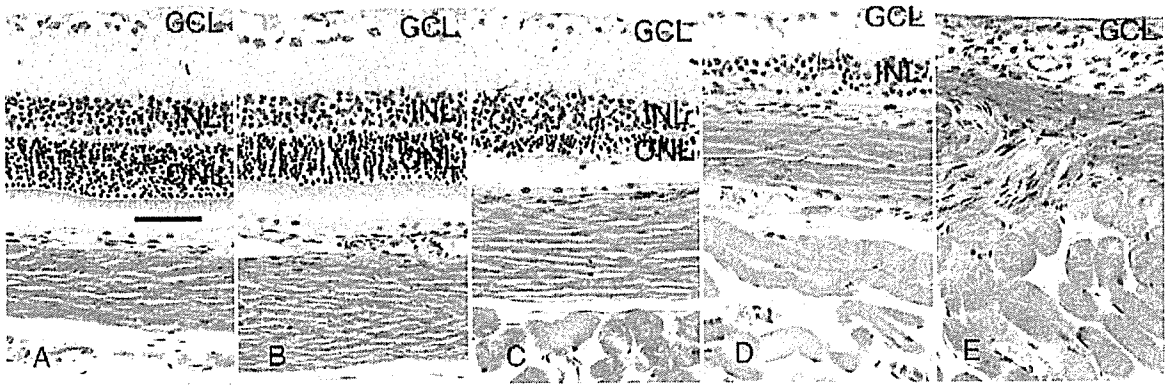

Fig. 3 – Representative microphotographs of histological examination by hematoxylin and eosin staining in rat retina 2 weeks after treatment of each dose of cobalt chloride. (A) 5, (B) 15, (C) 50, (D) 150 and (E) 500 nmol cobalt chloride in 5 μl of distilled water was injected intravitreally. As described in Results, the cobalt-chloride-induced morphological changes in each retina were scored semi-quantitatively. In panel A, no morphological change was recognized, thus scored 0. The morphological changes of retinal cell degeneration in panels B, C, D and E were scored 1, 2, 3 and 4, respectively. GCL, ganglion cell layer; INL, inner nuclear layer; ONL, outer nuclear layer. Scale bar in panel A, 50 μm.

the retinal area showing selective photoreceptor cell degeneration to all the retinal area. Total retina damage rate (TDR) was defined as the ratio of the retinal area showing the damage of total retinal layer to all the retinal area. RDI was used for the time course analysis for mouse retina, and dose–response analyses for mouse and rat retina. PDR and TDR rate was used for the dose–response analyses for mouse and rat retina.

2.2. *Apoptotic evaluation of the retinal degeneration*

The nuclear DNA fragmentation recognized as brown stain in ONL by in situ terminal dUTP-biotin nick end labeling of DNA fragments (TUNEL) method (Fig. 2) was scored semi-quantitatively by microscopic examination as follows: negative, 0; less than 50% of apoptotic cells in ONL, 1; more than 50% of apoptotic cells in ONL, 2; and apoptotic cells recognized as total retinal damage, 3. Most severe apoptotic lesion was evaluated and scored in each retina. The mean score of each group was defined as retinal apoptotic index (RAI). RAI was used for the time course analysis for mouse retina. In the mouse retina showing selective photoreceptor cell degeneration, TUNEL-positive cells were detected exclusively in the ONL. At 48 h after the injection of 12 nmol cobalt chloride, the RAI reached a peak.

2.3. *Dose–response analysis for mouse retina*

Dose–response increase of RDI in mouse retina was shown by intravitreal injection of cobalt chloride (Fig. 4A). PDR gradually increased dose-dependently and peaked at 10 nmol treatment. At 20 nmol treatment, PDR decreased and TDR increased (Fig. 4B). This means that suitable concentration for the induction of selective photoreceptor cell degeneration is 10 nmol cobalt chloride in mouse retina. Under these conditions, the photoreceptor outer segments were totally absent and the ONL could not be identified. In contrast, ganglion cell layer and inner nuclear layer were well preserved (Fig. 1D). This retinal morphology resembles the retinal degeneration that occurs in the mutant *rd* mouse.

2.4. *Time course analysis for mouse retina*

The results of the time course analysis for mouse retina at the dose of 12 nmol and 18 nmol of cobalt chloride are presented in Figs. 5A and B, respectively. At the dose of 12 nmol cobalt chloride, there was no retinal damage at 12 and 24 h after intravitreal injection. RDI increased from 48 h after injection and the retinal damage was complete at 1 week after injection. At the dose of 18 nmol cobalt chloride, RDI increased from 24 h after injection and the retinal damage was complete at 1 week after injection. RDI at 2 and 4 weeks were stable at both doses of cobalt chloride. This means the damaged lesions were irreversible. More severe lesions were seen at 18 nmol compared with that of 12 nmol cobalt chloride. The TUNEL-positive cells preceded morphological cell damage in ONL and RAI peaked at 48 h after the drug injection (Figs. 5A and B).

2.5. *Dose–response analysis for rat retina*

Dose–response increase of RDI in rat retina was also shown in the same manner of mouse by intravitreal injection of cobalt chloride (Fig. 6A). PDR gradually increased dose-dependently and peaked at 50 nmol cobalt chloride (Fig. 6B). Severe retinal damages occurred at 150 and 500 nmol (Fig. 6B). At the concentration for the induction of selective photoreceptor cell degeneration, the photoreceptor outer segments were totally absent and the ONL could not be identified (Fig. 3D). In contrast, ganglion cell layer and inner nuclear layer were well preserved.

3. Discussion

Although it is well known that the retina is one of the most metabolically active tissues in the body and oxygen is known to be the most supply-limited metabolite in the retina (Trick and Berkowitz, 2005), possible roles of the metabolic

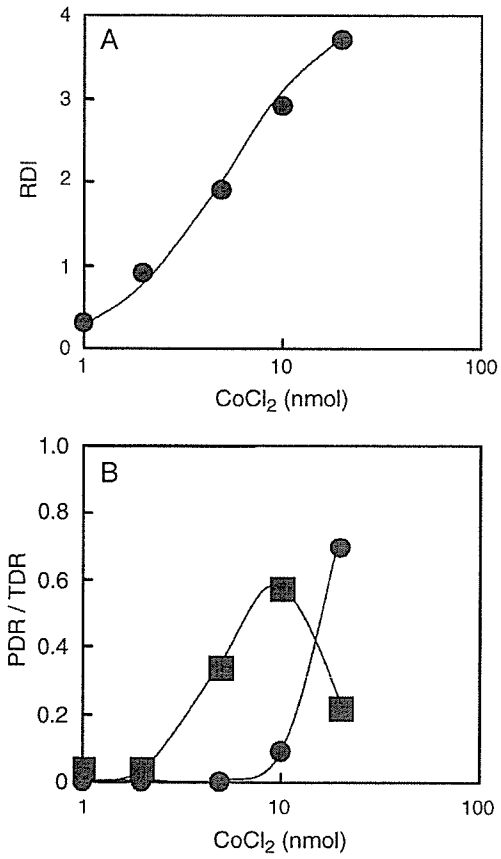

Fig. 4 – Dose–response analysis of mouse retinal damage 2 weeks after intravitreal injection at each dose of cobalt chloride. As described in Results, the cobalt-chloride-induced morphological changes in each retina was scored semi-quantitatively. The mean score of each group of cobalt-chloride-treated retina was defined as RDI. PDR was defined as the ratio of the retinal area showing selective photoreceptor cell degeneration to all the retinal area. TDR was defined as the ratio of the retinal area showing the damage of total retinal layer to all the retinal area. RDI (●) is plotted in panel A, and PDR (■) and TDR (●) are plotted in panel B. RDI, retinal damage index; PDR, photoreceptor damage rate; TDR, total retina damage rate.

microenvironment of the retina in the retinal degenerative process have not been clarified yet (Yu and Cringle, 2005). Because a continuous supply of oxygen is necessary to maintain retinal function, oxygen deprivation results in significant and permanent retinal dysfunction. In animal mutant models of photoreceptor degeneration, manipulation of environmental oxygen levels has been reported to be able to modulate the rate of photoreceptor degeneration (Maslim et al., 1997; Valter et al., 1998). Metabolic changes within the retina in the early phase of degenerative process may also contribute to the further progression of photoreceptor cell loss (Yu and Cringle, 2005; Yu et al., 2005).

In the present study, retinal photoreceptor cell degeneration was induced by cobalt chloride, which provides chemically induced hypoxia-mimicking conditions, both in mice and in rats. Photoreceptor cells progressively degenerated with time and dose dependency. The ONL-specific photoreceptor cell degeneration was induced by intravitreal injection of cobalt chloride, at 10–12 nmol in mice and 50 nmol in rats. The retinal morphology of the mice observed 2 weeks after the cobalt chloride injection resembles retinal degeneration seen in the mutant *rd* mouse. The photoreceptor cell degeneration can be produced by cobalt chloride without use of the retinal degeneration mutant animals.

Cobalt chloride has been widely used as a hypoxia-mimicking agent in both in vivo (Badr et al., 1999) and in vitro studies (Wang and Semenza, 1993).

The hypoxia-responsive pathway is specifically stimulated by exposure to cobalt chloride, which acts in the presence of oxygen without inhibition of oxidative phosphorylation (Badr et al., 1999). Cobalt chloride is a bioactive chemical. For example, it plays a critical role in the synthesis of vitamin B12. And it acts as a hypoxia-mimicking agent leading to enhanced expression of a set of hypoxia-responsive genes (Vengellur and LaPres, 2004; Vengellur et al., 2003). Many reports have shown that both cobalt and hypoxia regulate a similar group of genes on a global gene expression level (Ji et

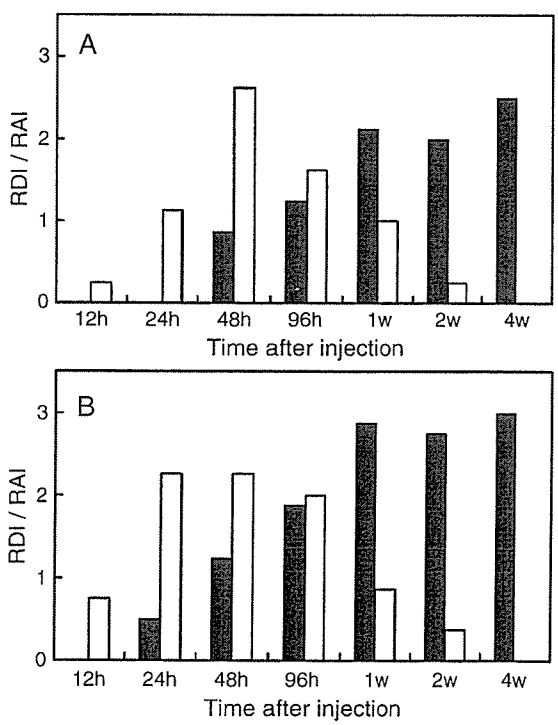

Fig. 5 – Time course of retinal damage detected by hematoxylin and eosin (HE) staining and TUNEL method at the dose of 12 nmol (A) and 18 nmol of cobalt chloride (B). As described in Results, the cobalt-chloride-induced morphological changes in each retina were scored semi-quantitatively and the TUNEL-positive apoptotic cells in ONL were also scored semi-quantitatively. The mean score of HE staining in each group of cobalt-chloride-treated retina was defined as RDI. The mean TUNEL score of each group was defined as RAI. RDI, retinal damage index; RAI, retinal apoptotic index. ■, RDI; □, RAI.

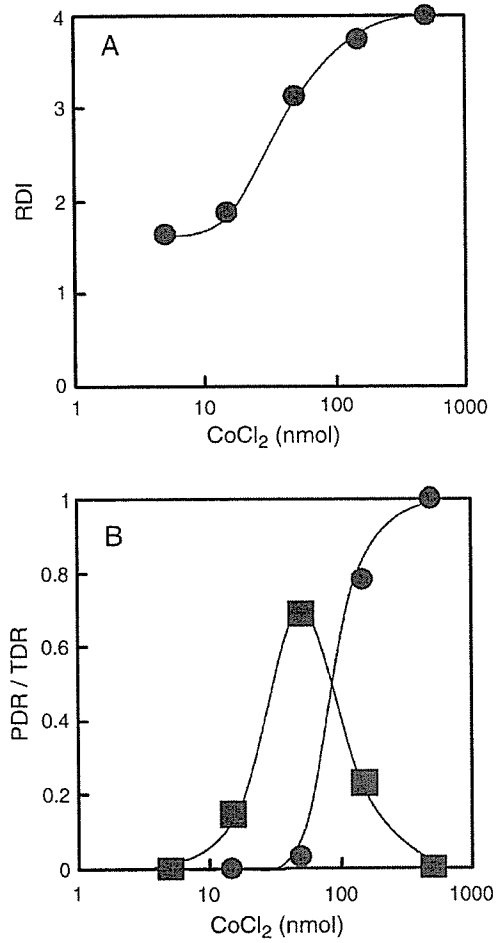

Fig. 6 – Dose–response analysis of rat retinal damage 2 weeks after intravitreal injection at each dose of cobalt chloride. As described in Results, the cobalt-chloride-induced morphological changes in each retina were scored semi-quantitatively. RDI (●) is plotted in panel A, and PDR (■) and TDR (●) are plotted in panel B. RDI, retinal damage index; PDR, photoreceptor damage rate; TDR, total retina damage rate.

al., in press; Lee et al., 2001; Vengellur et al., 2003). In rat cerebrum and retina, exposure to cobalt chloride, presumably acting through the hypoxia-signaling pathway including hypoxia-inducible factors, results in enhanced expression of major glucose transporter associated proteins, without increasing the capillary density (Badr et al., 1999). Furthermore, many reports demonstrated that cobalt chloride could induce apoptosis in many different kinds of cells. For examples, cobalt chloride was shown to induce apoptosis in rat C6 glioma cells (Yang et al., 2004), human alveolar macrophages (Araya et al., 2002), neuronal PC12 cells (Zou et al., 2001) and HeLa human cervical cancer cells (Kim et al., 2003). Our results also demonstrated that cobalt chloride is an apotopsis-inducing agent before retinal degeneration, which acts specifically in the photoreceptor cells.

Although an excessive dose of cobalt chloride damaged total retinal layers at an appropriate dose, cobalt chloride induced the selective photoreceptor cell degeneration with the well-preserved inner retina in both mice and rats. Oxygen supply to the retina is derived from two separate vascular systems. The choroid provides oxygen to the outer retina, while the retinal circulation provides the oxygen requirements of the inner retina. The retinal circulation is relatively sparse (presumably to allow passage of light to the photoreceptors), however, the choroid is highly vascularized. The extremely high oxygen consumption occurs in the inner segments of the photoreceptors, which are supplied from the vascular-rich choroid (Yu and Cringle, 2005). Thus, photoreceptor cells are considered more vulnerable than any other retinal cells to hypoxia-mimicking conditions induced by intravitreal injection of cobalt chloride. Interestingly, the adult rat retina is vulnerable to both hypoxia (air with the concentration of oxygen at 10%) and hyperoxia (45%, 65%, 70% and 75%) examined under real oxygen condition (Wellard et al., 2005). The vulnerability under the conditions is also specific to photoreceptors, and other retinal neurons have appeared resistant to the oxygen levels (Wellard et al., 2005).

The retina is an essential neural compartment and is used experimentally for understanding the development of the central nervous system (Hara et al., 2004b; Jones and Marc, 2005). Thus, it is hoped that the results from animal models of hypoxia-related retinal degeneration could provide relevant information for improving strategies for therapeutic intervention in ischemic insults of the human central nervous system. A number of reviews deal with the genetic aspects of retinal degeneration (Berson, 1993; Dryja and Berson, 1995), but there is much less known about the environmental and metabolic aspects, especially oxygen environment in the retinal degenerative process. Hyperoxia has been used to treat retinal degeneration clinically. Significant improvements have been reported in the electrophysiological responses in the treatment of retinitis pigmentosa patients with hyperbaric oxygen therapy (Vingolo et al., 1998).

In inner retina, intravitreal injection of N-methyl-D-aspartate (NMDA), a glutamate receptor agonist, is a good model for in vivo neuronal degeneration since glutamate-induced excitotoxicity is associated with a selective loss of retinal neurons after retinal ischemia and possibly in glaucoma (Kumada et al., 2004, 2005). Glutamate, or related excitatory amino acids, is thought to mediate excitatory synaptic transmission acting through activation of glutamate receptors (Sucher et al., 1997). Since glutamate is probably the excitatory transmitter used by retinal ganglion cells, the intravitreal NMDA injection model seems to be based on the intrinsic system of synaptic transmission.

In the present study, intravitreal injection of cobalt chloride, which provides chemically induced hypoxia-mimicking conditions, is also considered a good model for in vivo retinal photoreceptor degeneration because of the vulnerability of photoreceptor cells to oxygen environment in the degenerative process. On the other hand, the retinal morphology observed 2 weeks after the cobalt chloride injection resembles the retinal degeneration that occurs in the mutant *rd* mouse. This suggests that the photoreceptor cell degenerations in both the genetic aspects and the

metabolic aspects are based on a similar cytological process. In fact, apoptosis is the final common pathway and precedes the morphological changes of photoreceptor cells in many cases of retinal degeneration.

In addition to the model for the vulnerability of photoreceptor cells to oxygen environment in the degenerative process, cobalt-chloride-treated animal can be used as a recipient for tissue regeneration model. Usually, rd mouse is utilized as a recipient animal to assess the capacity for the grafted neural progenitor cells (Lu et al., 2002) or embryonic stem cells (Meyer et al., 2004). Our model can be also used as a recipient animal for tissue regeneration without use of the animals possessing gene mutations. Further studies are necessary to clarify the roles of cobalt chloride in expression of hypoxia-responsive genes in retina and the applications of cobalt-chloride-treated retina in the research of tissue regeneration.

4. Experimental procedures

4.1. *Animals*

Male ddY mice (6–7 weeks) were purchased from a local supplier (Chubukagakusizai, Co., Japan) and maintained under 12 h light:12 h dark cyclic lighting conditions. Male Wistar rats (6–7 weeks) were also purchased from the same supplier and maintained under the same conditions.

4.2. *Intravitreal injection to mice*

The method to inject cobalt chloride solution was performed with some modifications to the method by Timmers et al. (2001). Mice were anesthetized with intraperitoneal injection of 50 mg/kg sodium pentobarbital (Nembutal, Dainippon Pharmaceutical. Co. Ltd., Japan). Animals were placed in the pronate position under the SN MD-II operation microscope (Nagashima Medical Instruments Co., LTD, Japan). Pupils were then dilated with one drop of 0.5% phenylephrine hydrochloride–0.5% tropicamide solution (Mydrin P, Santen Pharmaceutical, Japan). Topical anesthetics were performed with one drop of 0.4% oxybuprocaine (Benoxil, Santen Pharmaceutical, Japan). Mouse fundus was visualized with a drop of 1.5% hydroxycellulose (SCOPISOL15, Senju Pharmaceutical, Japan) to the eye. The cornea was carefully punctured nasally approximately 0.5 mm medial to the dilated papillary margin using a 30-gauge hypodermic needle (Becton Dickinson and Company, NJ). The needle was advanced through the cornea into the anterior chamber and then injected 2 μl of hyaluronate sodium (Healon, Pfizer Pharmaceutical, NY or VISCORT, Alcon, TX) along the inside of the cornea. Then, 33-gauge blunt needle (Hamilton Company, NV) was inserted through the corneal puncture and advanced into anterior chamber, avoiding trauma to the iris and lens. Subsequently, needle shaft was aimed to posterior chamber, lateral from iris and medial toward lens. The lens was displaced medially as the needle was advanced to the surface of retina through the vitreous cavity. When the tip of the needle reached to the desired injection location, 2 μl of cobalt chloride solution was injected slowly and keep the position approximately 30 s. The viscosity of the hyaluronate sodium placed in anterior chamber avoids a small amount of reflux of injected material through the corneal wound.

4.3. *Intravitreal injection to rats*

The method to inject cobalt chloride solution was performed with the same method as mice. Rats were anesthetized and placed in the pronate position under the SN MD-II operation microscope. Pupils were dilated with one drop of 0.5% phenylephrine hydrochloride–0.5% tropicamide solution, and topical anesthetics were performed with one drop of 0.4% oxybuprocaine. Rat fundus was visualized with a drop of 1.5% hydroxycellulose to the eye. The cornea was punctured nasally approximately 0.7 mm medial to the dilated papillary margin using a 30-gauge hypodermic needle. The needle was advanced through the cornea into the anterior chamber and then injected 5 μl of hyaluronate sodium along the inside of the cornea. Then, 33-gauge blunt needle was inserted through the corneal puncture. When the tip of the needle reached to the desired injection location, 5 μl of cobalt chloride solution was injected slowly and keep the position approximately 30 s in the same manner as mice.

4.4. *Dose–response analysis for mouse retina*

Five doses of cobalt chloride solution, 1, 2, 5, 10 and 20 nmol in 2 μl of distilled water, have been used for the dose–response study. The whole eyes were extracted at 2 weeks after intravitreal injection. Ten eyes per group were used for the experiment.

4.5. *Time course analysis for mouse retina*

The whole eyes were extracted at 0, 12, 48 and 96 h and 1, 2 and 4 weeks after intravitreal cobalt chloride injection. Two doses (12 nmol and 18 nmol) of cobalt chloride solution have been used for this study. Eight eyes per group were used for the experiment.

4.6. *Dose–response analysis for rat retina*

Five doses of cobalt chloride solution, 5, 15, 50, 150 and 500 nmol in 5 μl of distilled water, have been used for the dose–response study. The whole eyes were extracted at 2 weeks after intravitreal injection. Eight eyes per group were used for the experiment.

4.7. *Histologic processing*

The mice and rats were killed with an overdose of pentobarbital sodium. The specimens were fixed overnight in 10% phosphate-buffered formalin by setting on a mixing machine (MildMixer PR-36; TAITEC, Tokyo, Japan) and then embedded in paraffin. Two sequential sections were cut as 3 μm along vertical meridian through the optic nerve, placed on poly-L-lysine-coated microscopic slides and then used for HE staining and TUNEL method.

4.8. TUNEL method

TUNEL method was performed as described previously (Hara et al., 2004a; Kumada et al., 2005). After incubation with 20 mg/ml proteinase K (Sigma), the serial sections used for HE staining were immersed in TDT buffer (30 mM Trizma base, pH 7.2, 140 mM sodium cacodylate, 1 mM cobalt chloride). TDT (Boehringer Mannheim GmbH, Mannheim, Germany) and biotinylated dUTP (Boehringer Mannheim GmbH, Mannheim, Germany) were diluted in TDT buffer at a concentration of 0.15 e.u./ml and 0.8 nmol/ml, respectively. The solution was placed on the sections and then incubated at 37 °C for 60 min. The sections were covered with streptavidin peroxidase (DAKO, Carpinteria, USA) and stained with 3,3′-diaminobenzidine (DAB) as a substrate for the peroxidase. Finally, counterstaining was done using Mayer's hematoxylin.

REFERENCES

Araya, J., Maruyama, M., Inoue, A., Fujita, T., Kawahara, J., Sassa, K., Hayashi, R., Kawagishi, Y., Yamashita, N., Sugiyama, E., Kobayashi, M., 2002. Inhibition of proteasome activity is involved in cobalt-induced apoptosis of human alveolar macrophages. Am. J. Physiol.: Lung Cell. Mol. Physiol. 283, L849–L858.

Badr, G.A., Zhang, J.Z., Tang, J., Kern, T.S., Ismail-Beigi, F., 1999. Glut1 and glut3 expression, but not capillary density, is increased by cobalt chloride in rat cerebrum and retina. Brain Res. Mol. Brain Res. 64, 24–33.

Berson, E.L., 1993. Retinitis pigmentosa. The Friedenwald Lecture. Invest. Ophthalmol. Visual Sci. 34, 1659–1676.

Bowes, C., Li, T., Danciger, M., Baxter, L.C., Applebury, M.L., Farber, D.B., 1990. Retinal degeneration in the rd mouse is caused by a defect in the beta subunit of rod cGMP-phosphodiesterase. Nature 347, 677–680.

Chang, B., Heckenlively, J.R., Hawes, N.L., Roderick, T.H., 1993. New mouse primary retinal degeneration (rd-3). Genomics 16, 45–49.

Delyfer, M.N., Leveillard, T., Mohand-Said, S., Hicks, D., Picaud, S., Sahel, J.A., 2004. Inherited retinal degenerations: therapeutic prospects. Biol. Cell 96, 261–269.

Dryja, T.P., Berson, E.L., 1995. Retinitis pigmentosa and allied diseases. Implications of genetic heterogeneity. Invest. Ophthalmol. Visual Sci. 36, 1197–1200.

Green, W.R., 1999. Histopathology of age-related macular degeneration. Mol. Vision 5, 27.

Hara, A., Niwa, M., Kumada, M., Kitaori, N., Yamamoto, T., Kozawa, O., Mori, H., 2004a. Fragmented DNA transport in dendrites of retinal neurons during apoptotic cell death. Brain Res. 1007, 183–187.

Hara, A., Niwa, M., Kunisada, T., Yoshimura, N., Katayama, M., Kozawa, O., Mori, H., 2004b. Embryonic stem cells are capable of generating a neuronal network in the adult mouse retina. Brain Res. 999, 216–221.

Hawes, N.L., Chang, B., Hageman, G.S., Nusinowitz, S., Nishina, P.M., Schneider, B.S., Smith, R.S., Roderick, T.H., Davisson, M.T., Heckenlively, J.R., 2000. Retinal degeneration 6 (rd6): a new mouse model for human retinitis punctata albescens. Invest. Ophthalmol. Visual Sci. 41, 3149–3157.

Ji, Z., Yang, G., Shahzidi, S., Tkacz-Stachowska, K., Suo, Z., Nesland, J.M., Peng, Q., in press. Induction of hypoxia-inducible factor-1alpha overexpression by cobalt chloride enhances cellular resistance to photodynamic therapy. Cancer Lett.

Jimenez, A.J., Garcia-Fernandez, J.M., Gonzalez, B., Foster, R.G., 1996. The spatio-temporal pattern of photoreceptor degeneration in the aged rd/rd mouse retina. Cell Tissue Res. 284, 193–202.

Jones, B.W., Marc, R.E., 2005. Retinal remodeling during retinal degeneration. Exp. Eye Res. 81, 123–137.

Kennan, A., Aherne, A., Humphries, P., 2005. Light in retinitis pigmentosa. Trends Genet. 21, 103–110.

Kim, H.J., Yang, S.J., Kim, Y.S., Kim, T.U., 2003. Cobalt chloride-induced apoptosis and extracellular signal-regulated protein kinase activation in human cervical cancer HeLa cells. J. Biochem. Mol. Biol. 36, 468–474.

Kumada, M., Niwa, M., Wang, X., Matsuno, H., Hara, A., Mori, H., Matsuo, O., Yamamoto, T., Kozawa, O., 2004. Endogenous tissue type plasminogen activator facilitates NMDA-induced retinal damage. Toxicol. Appl. Pharmacol. 200, 48–53.

Kumada, M., Niwa, M., Hara, A., Matsuno, H., Mori, H., Ueshima, S., Matsuo, O., Yamamoto, T., Kozawa, O., 2005. Tissue type plasminogen activator facilitates NMDA-receptor-mediated retinal apoptosis through an independent fibrinolytic cascade. Invest. Ophthalmol. Visual Sci. 46, 1504–1507.

Lee, S.G., Lee, H., Rho, H.M., 2001. Transcriptional repression of the human p53 gene by cobalt chloride mimicking hypoxia. FEBS Lett. 507, 259–263.

Lu, B., Kwan, T., Kurimoto, Y., Shatos, M., Lund, R.D., Young, M.J., 2002. Transplantation of EGF-responsive neurospheres from GFP transgenic mice into the eyes of rd mice. Brain Res. 943, 292–300.

Maslim, J., Valter, K., Egensperger, R., Hollander, H., Stone, J., 1997. Tissue oxygen during a critical developmental period controls the death and survival of photoreceptors. Invest. Ophthalmol. Visual Sci. 38, 1667–1677.

Meyer, J.S., Katz, M.L., Maruniak, J.A., Kirk, M.D., 2004. Neural differentiation of mouse embryonic stem cells in vitro and after transplantation into eyes of mutant mice with rapid retinal degeneration. Brain Res. 1014, 131–144.

Roessner, C.A., Santander, P.J., Scott, A.I., 2001. Multiple biosynthetic pathways for vitamin B12: variations on a central theme. Vitam. Horm. 61, 267–297.

Sucher, N.J., Lipton, S.A., Dreyer, E.B., 1997. Molecular basis of glutamate toxicity in retinal ganglion cells. Vision Res. 37, 3483–3493.

Timmers, A.M., Zhang, H., Squitieri, A., Gonzalez-Pola, C., 2001. Subretinal injections in rodent eyes: effects on electrophysiology and histology of rat retina. Mol. Vision 7, 131–137.

Trick, G.L., Berkowitz, B.A., 2005. Retinal oxygenation response and retinopathy. Prog. Retinal Eye Res. 24, 259–274.

Valter, K., Maslim, J., Bowers, F., Stone, J., 1998. Photoreceptor dystrophy in the RCS rat: roles of oxygen, debris, and bFGF. Invest. Ophthalmol. Visual Sci. 39, 2427–2442.

Vengellur, A., LaPres, J.J., 2004. The role of hypoxia inducible factor 1alpha in cobalt chloride induced cell death in mouse embryonic fibroblasts. Toxicol. Sci. 82, 638–646.

Vengellur, A., Woods, B.G., Ryan, H.E., Johnson, R.S., LaPres, J.J., 2003. Gene expression profiling of the hypoxia signaling pathway in hypoxia-inducible factor 1alpha null mouse embryonic fibroblasts. Gene Expression 11, 181–197.

Vingolo, E.M., Pelaia, P., Forte, R., Rocco, M., Giusti, C., Rispoli, E., 1998. Does hyperbaric oxygen (HBO) delivery rescue retinal photoreceptors in retinitis pigmentosa? Doc. Ophthalmol. 97, 33–39.

Wang, G.L., Semenza, G.L., 1993. Desferrioxamine induces erythropoietin gene expression and hypoxia-inducible factor 1 DNA-binding activity: implications for models of hypoxia signal transduction. Blood 82, 3610–3615.

Wellard, J., Lee, D., Valter, K., Stone, J., 2005. Photoreceptors in the rat retina are specifically vulnerable to both hypoxia and hyperoxia. Vis. Neurosci. 22, 501–507.

Yang, S.J., Pyen, J., Lee, I., Lee, H., Kim, Y., Kim, T., 2004. Cobalt

chloride-induced apoptosis and extracellular signal-regulated protein kinase 1/2 activation in rat C6 glioma cells. J. Biochem. Mol. Biol. 37, 480–486.

Yu, D.Y., Cringle, S.J., 2005. Retinal degeneration and local oxygen metabolism. Exp. Eye Res. 80, 745–751.

Yu, D.Y., Cringle, S.J., Su, E.N., 2005. Intraretinal oxygen distribution in the monkey retina and the response to systemic hyperoxia. Invest. Ophthalmol. Visual Sci. 46, 4728–4733.

Zack, D.J., Dean, M., Molday, R.S., Nathans, J., Redmond, T.M., Stone, E.M., Swaroop, A., Valle, D., Weber, B.H., 1999. What can we learn about age-related macular degeneration from other retinal diseases? Mol. Vision 5, 30.

Zou, W., Yan, M., Xu, W., Huo, H., Sun, L., Zheng, Z., Liu, X., 2001. Cobalt chloride induces PC12 cells apoptosis through reactive oxygen species and accompanied by AP-1 activation. J. Neurosci. Res. 64, 646–653.

A pilot study to detect glaucoma with confocal scanning laser ophthalmoscopy compared to nonmydriatic stereoscopic photography in a community health screening

Authors: Shinji Ohkubo, MD, PhD, Hisashi Takeda, MD, PhD,
Tomomi Higashide, MD, PhD, Tsugihisa Sasaki, MD, PhD,
and Kazuhisa Sugiyama, MD, PhD

Affiliations: Department of Ophthalmology, Kanazawa University Graduate School of Medical Science, Kanazawa, Japan

Correspondence: Shinji Ohkubo, MD, PhD
Department of Ophthalmology, Kanazawa University Graduate School of Medical Science,
13-1 Takara-machi, Kanazawa, Ishikawa 9208641 Japan,
Telephone: 81-76-265-2403, Fax: 81-76-222-9660
E-mail address: eyeshin@med.kanazawa-u.ac.jp

No author of this manuscript had a proprietary or financial interest in it.

Abstract

Purpose: To assess the efficacy and practical usefulness of the Heidelberg Retina Tomograph II (HRT II) compared with nonmydriatic stereoscopic photography in a public glaucoma screening.

Methods: We examined 1,173 local residents, aged 40 years or older, who visited a community health screening in Komatsu City. Initial glaucoma screening consisted of non-contact pneumotonometry, nonmydriatic stereoscopic fundus photography and HRT II. When glaucoma was suspected, the subjects were referred for a definitive examination, in which slit-lamp biomicroscopic examination, Goldmann applanation tonometry, Humphrey 30-2 test, gonioscopy, and optic nerve head evaluation were performed.

Results: A total of 97.2% (2279/2345) of the nonmydriatic stereoscopic optic disc photographs could be interpreted and 93.4% (2189/2345) were good images. HRT II measurements were successful in 99.0% (2322/2345) of eyes, and acceptable images were obtained in 91.9% (2154/2345) of eyes. Based on clinical diagnoses, 94 eyes of 60 participants were diagnosed with glaucoma. The sensitivity of nonmydriatic stereoscopic photographs for personal-level analysis and eye-level analysis was 95.8% and 95.5%, respectively. Using Moorfield's regression analysis, HRT sensitivity and specificity were 72.3% to 91.5% and 84.0% to 93.1%, respectively, for personal-level analysis, and 60.3% to

72.6% and 89.7% to 95.6%, respectively, for eye-level analysis.

Conclusion: Although HRT II did not detect glaucoma as well as optic nerve stereophotographs in this Japanese population, it may play a role in community health screening.

Key Words: Heidelberg Retina Tomograph II; nonmydriatic stereoscopic photography; public glaucoma screening

INTRODUCTION

More than 50% of glaucoma patients remain undiagnosed in the United States[1] and Europe.[2] Recently, a Japanese population screening study[3] revealed that the prevalence of primary open-angle glaucoma (POAG) in the Japanese population older than 40 years was estimated to be 3.9%, of which 93.3% of POAG patients were previously undiagnosed. Therefore, a mass screening method for glaucoma is urgently needed. Three-dimensional evaluation of the optic disc by glaucoma specialists is thought to be the ideal method but subjective techniques are routinely used to evaluate the optic disc and retinal nerve fiber layer (RNFL), and test results clearly depend on the examiner's experience. Consequently, it would be useful to introduce objective quantitative measurements. Recently, a number of new devices have been developed for this purpose[4-7], including the Heidelberg Retina Tomograph II (HRT II; Heidelberg Instruments, Heidelberg, Germany), a confocal scanning laser ophthalmoscope that allows a rapid three-dimensional topographic analysis of the optic disc and retina without pupillary dilatation.

The purpose of this study was to investigate the efficacy and practical usefulness of the HRT II compared with nonmydriatic stereoscopic photography in a public glaucoma screening.

Subjects and Methods

Study Population

This study was approved by the Ethical Committee of Kanazawa University Graduate School of Medical Science. Subjects were recruited at an annual community health screening project in Komatsu City, Japan, conducted from June 2003 to July 2003. To be eligible to participate in the health checkup, a citizen must be older than 40 years and without an opportunity to receive a health checkup at an office. At the checkup, we posted a bill about glaucoma screening at the building entrance and arranged to use a venue nearby. Three thousand subjects participated in the community health checkup, of which 1,173 subjects participated in the glaucoma screening. Written informed consent was obtained from all participants in the study.

Initial Screening Examination

The screening methods used in this study were implemented in two stages. After obtaining informed consent, an initial screening was performed, which included recording of personal data (sex, age, personal and family histories of glaucoma, systemic and local disease, and subjective ocular symptoms), autorefractometry, tonometry, digital nonmydriatic

stereoscopic photography and HRT II.

Intraocular pressure (IOP) was measured using non-contact pneumotonometry (NCT) (Canon, TX-F, Tokyo, Japan). Refractive status was measured using an autorefractometer (Nidek, ARK-730A, Gamagori, Japan). Nonsimultaneous 30°-field stereoscopic digital color images of optic nerve heads were obtained without pupillary dilatation using the IMAGEnet digital fundus camera system (Topcon, NSW6S, Tokyo, Japan). Two sequential photographs of each eye were taken, with a lateral shift in camera position to obtain a stereo effect. All participants underwent imaging (scanning field, 15° × 15°) with an HRT II. All images were obtained by one of two trained technicians. Magnification errors were corrected using patients' corneal curvature measurements. The contour line of the optic disc edge was drawn by consensus between two of the authors (SO, HT) while viewing stereoscopic photographs of the optic disc.

Evaluation of Optic Nerve Head

The optic nerve was evaluated from nonsimultaneous stereoscopic digital photographs of the optic disc using a 3D Viewer System (Topcon, 3D Viewer and Stereo Viewer System, Tokyo, Japan), which consisted of electronic shutter glasses (StereoGraphics Corp., Crystal Eyes 3, San Rafael, CA, USA), an emitter (StereoGraphics Corp., E-2), and a 19-inch flat

screen monitor (Nanao, T766, Matto, Japan). The photographic quality was classified as "good quality", "poor quality" or "not available". "Poor quality" was when obtaining a stereo view failed or was poor, but still assessable. The subjects with poor quality stereoscopic photographs were referred for a definitive examination except those were judged to be obviously normal by monoscopic fundus photography.

HRT II Confocal Scanning Laser Ophthalmoscopy

For every participant, three topographic images were obtained, combined and automatically aligned to generate one mean topographic image for analysis. Moorfield's regression analysis (MRA)[5], incorporated in the HRT II software (version 1.6), was applied for this screening. The imaging quality of HRT II was classified as "acceptable (topographic standard deviation ≤ 50□)", "unacceptable (topographic standard deviation > 50□)" or "not available".

Definitive Examination

A definitive examination was performed, masked to the initial screening results, when the subject was suspected to have glaucoma. The criteria for definitive examination eligibility are summarized in Table 1. When at least one finding suggested the presence of glaucoma,

the subjects were recruited for definitive examination.

In the definitive examination, slit-lamp biomicroscopic examination, Goldmann applanation tonometry, visual field test with a Humphrey Field Analyzer II 30-2 SITA Standard program (Carl Zeiss Meditec Inc., Dublin, CA, USA) and gonioscopy using a 4-mirror gonioscope (Menicon, PG-410, Nagoya, Japan) were performed. The pupil was dilated with 0.5% tropicamide and 0.5% phenylephrine hydrochloride and fundus examination was carried out with a slit lamp and super field NC lens (Volk Optical Inc., Mentor, OH, USA) or a 4-mirror gonioscope. Patients with occludable angles (20 subjects), or with driving responsibilities after the examination (3 subjects), were not dilated for this examination.

Evaluation of Visual Field

Two examiners evaluated the test results from the Humphrey Field Analyzer. We initially set the reliability criteria at fixation loss, ≤33%; false-positive and false-negative, ≤20%. However, only 73.7% (370 eyes) of the visual field data collected in the definitive examinations (502 eyes of 251 subjects) passed these criteria, so we applied the criteria in accordance with a recent Japanese population study (fixation loss, >50%; false-positive and false-negative, >50%). [3] Fifty-seven eyes (11.4%) failed these criteria. The criteria for

abnormal visual fields were based on a recent Japanese population study.[3] Briefly, abnormal visual field data was defined by the presence of at least one abnormal hemifield, which was determined by the criteria proposed by Anderson and Patella.[8] A hemifield was judged to be abnormal when the pattern deviation probability plot showed a cluster of 3 or more non-edge contiguous points, having sensitivity with a probability of less than 5% in the upper or lower hemifield, and in one of these, a probability of less than 1%.

Diagnosis of Glaucoma

A glaucoma specialist (KS) determined the final diagnosis on the basis of optic disc appearance, including nerve fiber layer defects, results of Humphrey Field Analyzer examinations, and clinical findings that were obtained through initial screening and definitive examinations. The criteria for glaucoma diagnosis were based on previous population studies[3, 9]. Category 1 glaucoma was diagnosed when the vertical cup/disc ratio of the optic nerve head was more than or equal to 0.7, or the rim width at the superior portion (11-1 hour) or inferior portion (5-7 hour) was less than or equal to 0.1 of disc diameter, or the difference in vertical cup/disc ratio was more than or equal to 0.2 between both eyes, or a nerve fiber layer defect was found, and the hemifield-based visual field abnormality was compatible with optic disc appearance or nerve fiber layer defect. When the visual field test

result was not reliable or available, category 2 glaucoma was diagnosed. This was where the vertical cup/disc ratio of the optic nerve head was more than or equal to 0.9, or the rim width at the superior portion (11-1 hour) or inferior portion (5-7 hour) was less than or equal to 0.05, or the difference in vertical cup/disc ratio was more than or equal to 0.3 between both eyes. Suspect glaucoma was diagnosed when the cup/disc ratio of the eye was 0.7 or more but less than 0.9, or the rim width at the superior portion (11-1 hour) or inferior portion (5-7 hour) was 0.1 or less but more than 0.05 of the disc diameter, or the difference in vertical cup/disc ratio was 0.2 or more but less than 0.3 between both eyes, or a nerve fiber layer defect was found, and the visual field test was not reliable or available or did not show a compatible hemifield-based defect. In definitive diagnosis, anomalous discs, including tilted discs and superior segmental optic hypoplasia, were carefully excluded. The glaucoma status of each person was classified on the basis of the more affected eye.

Main outcome Measures

To evaluate the practical usefulness of HRT II and nonmydriatic stereoscopic photography for mass screening, the imaging status of each instrument for each diagnostic category and by age were calculated. The grouping was performed for the HRT II examination results based on the MRA. "Borderline" outcomes were treated as test positive (only normal was

test negative, MRA 1) and "borderline" outcomes were treated as test negative (normal, borderline results were considered test negative, MRA 2). After these groupings, sensitivities, specificities, positive predictive value (PPV) and negative predictive value (NPV) for participants (person-level analysis) and for individual eyes (eye-level analysis), were calculated between the MRA diagnosis of HRT II and clinical diagnosis gold standards. Sensitivities of stereoscopic photographs for participants and for individual eyes were also calculated. Data from unacceptable topographic images, unacceptable photographs and subjects who did not undergo definitive examinations were excluded from this data analysis.

Data Analysis

The privacy of personal medical information was protected at the data analysis center of Kanazawa University Graduate School of Medical Science. Statistical analysis was performed using StatMate III software (ATMS, Tokyo, Japan). Differences between groups were evaluated using Student's t test. The chi-square test was used to compare proportions.

Results

The average age of all participants (435 male, 738 female) was 61.6±10.5 years

(mean ± standard deviation). Of the 1,173 subjects (2345 eyes) examined in the initial screening, 296 (25.2%) were referred for definitive examination, but 45 declined or were unable to participate. As a result, 251 subjects (84.8%) underwent definitive examination. Based on clinical diagnosis, 94 eyes of 60 participants were diagnosed with definite glaucoma and 41 eyes of 29 participants were diagnosed with suspect glaucoma. Following the definitive examination, diagnoses of six subjects were changed. One subject diagnosed with glaucoma was changed to superior segmental optic hypoplasia and one subject diagnosed with glaucoma was converted to suspect glaucoma. In addition, 4 subjects with suspect glaucoma were subsequently diagnosed as normal.

The rate of previously undiagnosed glaucoma was 90.0% (54/60). The number of primary open-angle glaucoma (POAG) subjects was 58. Of these, 55 subjects were diagnosed with category 1 criteria, and 3 were diagnosed with category 2 criteria. Of the 58 POAG subjects, 50 (86.2%) had an IOP of 21 mmHg or less without medication (both in initial screening and definitive examination in both eyes) and 8 had an IOP of more than 21 mmHg. No subjects were found to have primary angle-closure glaucoma. There were two secondary glaucoma subjects who were diagnosed with category 1 and exfoliation glaucoma. The average age of all glaucoma patients was 69.1±10.2 years (mean ± standard deviation). For the 45 subjects who did not undergo definitive examination,

diagnosis was based on the initial screening and 10 subjects met the criteria of category 2. However, these 45 subjects were excluded from the data analysis. Table 2 shows the age-specific prevalence of glaucoma in this screened population. The estimated prevalence of POAG and exfoliation glaucoma, was 5.1% (58/1128) (95% CI, 3.8%-6.4%) and 0.2% (2/1128) (95% CI, -0.1%-0.5%), respectively.

The imaging status of each instrument for each diagnostic category and by age is shown in Figure 1 and Table 3, respectively. The distribution of the quality of HRT II images obtained is shown in Figure 2. Figure 3 is a Venn diagram that summarizes the number of eyes that could not be interpreted by stereoscopic photography, those eyes that could not be scanned by HRT II, and both. Of the 66 eyes that could not be interpreted by stereoscopic optic disc photography, glaucoma was diagnosed in 21 eyes (31.8%). In the 23 eyes that could not be scanned by HRT II, glaucoma was diagnosed in 1 eye (4.3%). Figure 4 is a Venn diagram to show which eyes had poor quality stereoscopic photography, or unacceptable quality (above 50□m) HRT II, and both.

We reviewed the methods for detecting definitive glaucoma. When subjects with not available HRT II scans and not available stereoscopic photographs were considered along with subjects defined as test positive, glaucoma was detected in 58 subjects (58/60, 96.7%) by nonmydriatic stereoscopic photography, in 52 subjects (52/60, 86.7%) by HRT II